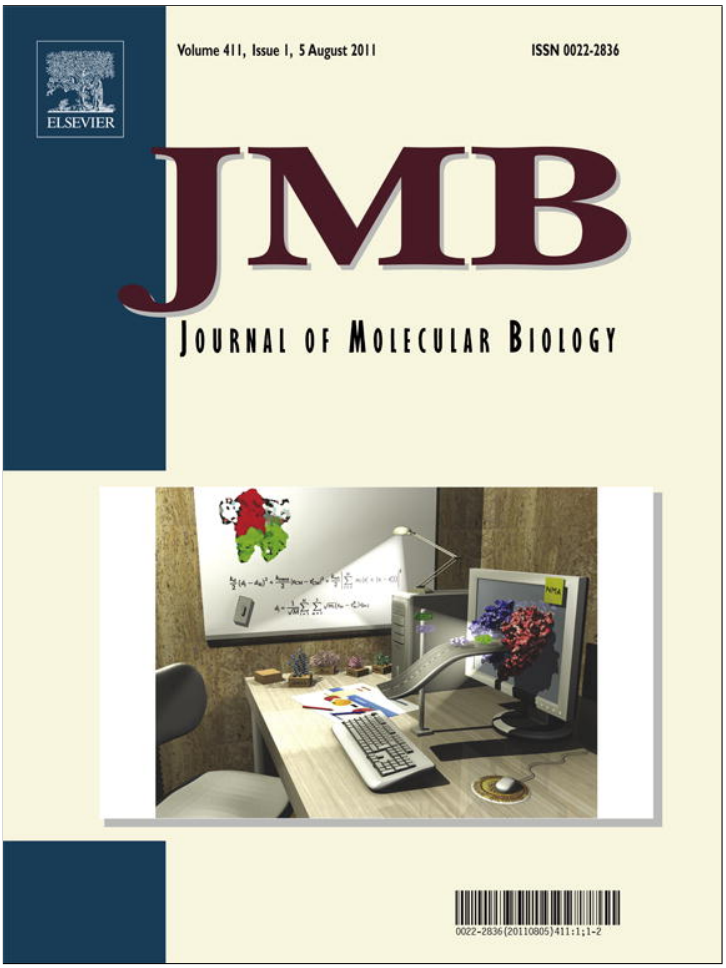

doi:10.1016/j.jmb.2011.05.037 J. Mol. Biol. (2011) 411, 53–67

Contents lists available at www.sciencedirect.com

Journal of Molecular Biology

journal homepage: http://ees.elsevier.com.jmb

# The Crystal Structure of the Substrate-Binding Protein OpuBC from *Bacillus subtilis* in Complex with Choline

**Marco Pittelkow[1]†, Britta Tschapek[2]†, Sander H. J. Smits[2], Lutz Schmitt[2]* and Erhard Bremer[1]***

[1]*Laboratory for Microbiology, Department of Biology, Philipps University Marburg, Karl-von-Frisch Str. 8, D-35032 Marburg, Germany*
[2]*Institute of Biochemistry, Heinrich Heine University Düsseldorf, Universitätsstr. 1, D-402325 Düsseldorf, Germany*

*Received 30 March 2011; received in revised form 17 May 2011; accepted 24 May 2011*
Available online 1 June 2011

***Edited by R. Huber***

***Keywords:***
ABC transporters; substrate-binding proteins; compatible solutes; choline; glycine betaine synthesis

*Bacillus subtilis* can synthesize the compatible solute glycine betaine as an osmoprotectant from an exogenous supply of the precursor choline. Import of choline is mediated by two osmotically inducible ABC transport systems: OpuB and OpuC. OpuC catalyzes the import of various osmoprotectants, whereas OpuB is highly specific for choline. OpuBC is the substrate-binding protein of the OpuB transporter, and we have analyzed the affinity of the OpuBC/choline complex by intrinsic tryptophan fluorescence and determined a $K_d$ value of about 30 μM. The X-ray crystal structure of the OpuBC/choline complex was solved at a resolution of 1.6 Å and revealed a fold typical of class II substrate-binding proteins. The positively charged trimethylammonium head group of choline is wedged into an aromatic cage formed by four tyrosine residues and is bound via cation–pi interactions. The hydroxyl group of choline protrudes out of this aromatic cage and makes a single interaction with residue Gln19. The substitution of this residue by Ala decreases choline binding affinity by approximately 15-fold. A water network stabilizes choline within its substrate-binding site and promotes indirect interactions between the two lobes of the OpuBC protein. Disruption of this intricate water network by site-directed mutagenesis of selected residues in OpuBC either strongly reduces choline binding affinity (between 18-fold and 25-fold) or abrogates ligand binding. The crystal structure of the OpuBC/choline complex provides a rational for the observed choline specificity of the OpuB ABC importer *in vivo* and explains its inability to catalyze the import of glycine betaine into osmotically stressed *B. subtilis* cells.



## Introduction

Changes in the osmotic conditions of the environment are key factors that influence the growth and survival of microorganisms in their different ecological niches.[1] Since most microorganisms possess turgor (an intracellular hydrostatic pressure considered to be essential for cell expansion and growth),[2] changes in external osmolarity inevitably trigger osmotically driven water fluxes across the semipermeable cytoplasmic membrane. The direction and magnitude of these water fluxes are determined by differences in the osmotic potential between the interior of the cell and the surroundings.[3,4]

Reduced cell growth and eventual growth arrest under severe high-osmolarity conditions are correlated

*Corresponding authors. E-mail addresses: lutz.schmitt@uni-duesseldorf.de; bremer@biologie.uni-marburg.de.

† M.P. and B.T. contributed equally to this work.

Abbreviations used: PDB, Protein Data Bank; JGI, Joint Genome Institute; MMA, minimal medium.

with a diminished content of free water in the cytoplasm of bacterial cells.[5] To counteract the efflux of water and to promote a physiologically adequate level of cellular hydration and turgor, many microorganisms amass a selected class of organic osmolytes, so-called compatible solutes, for a sustained adjustment to high-osmolarity surroundings.[1–4]

Glycine betaine, a trimethylated derivative of the amino acid glycine, is, without any doubt, the most widely used compatible solute in nature.[1,6–8] Many microbes that have been studied in the context of their adaptation to high-osmolarity environments have been found to possess high-affinity uptake systems for this compatible solute that are osmotically induced at the level of transcription and/or stimulated at the level of transport activity by osmotic-stress-derived cellular signals.[2–4,9,10] The three best mechanistically understood compatible solute transport systems are the BCCT-type carrier BetP from *Corynebacterium glutamicum*,[11,12] the ABC transporter OpuA from *Lactococcus lactis*,[13,14] and the MSF-type transporter ProP from *Escherichia coli*.[15]

Frequently, microorganisms can also synthesize glycine betaine and do so either via *de novo* synthesis or via oxidation of the precursor choline. *De novo* synthesis of glycine betaine is accomplished by a stepwise methylation of the amino acid glycine with *S*-adenosylmethionine as the methyl donor, a biosynthetic process that is energetically very costly due to the required regeneration of the cofactor.[16] Consequently, most microorganisms synthesize glycine betaine through an energetically less expensive pathway by first importing choline and the subsequent oxidation of this precursor molecule.[17–20] It should be noted in this context that choline has no osmoprotective property in microorganisms *per se*.[21]

*Bacillus subtilis* possesses three high-affinity uptake systems for glycine betaine: the ABC transporters OpuA and OpuC, and the BCCT-type transporter OpuD (Fig. 1).[22–24] The expression of structural genes for these transport systems is up-regulated in high-salinity-stressed *B. subtilis* cells,[25,26] thereby providing higher glycine betaine transport capacity. Glycine betaine can also be synthesized by *B. subtilis* from the precursor choline.[21] For this purpose, choline is imported with high affinity through the substrate-specific OpuB ABC transporter and the promiscuous ABC transporter OpuC (Fig. 1).[23,24,27–30] The imported choline is then oxidized to glycine betaine by the concerted actions of the alcohol dehydrogenase GbsB and the glycine betaine

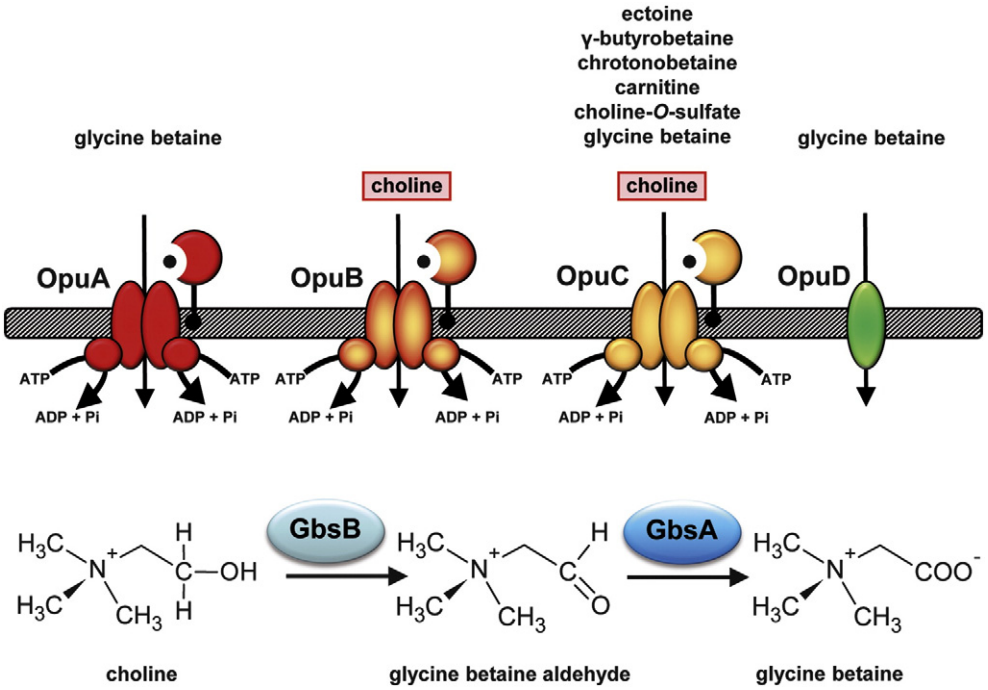


**Fig. 1.** The osmoprotectant uptake systems of *B. subtilis* and the synthesis pathway of glycine betaine from the precursor choline. The OpuA, OpuB, and OpuC osmoprotectant uptake (Opu) systems are members of the ABC family; the OpuD osmoprotectant uptake system is a member of the BCCT family. OpuAC, OpuBC, and OpuCC are extracellular solute receptors that are tethered to the outer face of the cytoplasmic membrane through lipid modification of an N-terminal Cys residue. The substrate specificities of the various Opu transporters have been previously assessed through osmoprotection growth assays and transport studies. The synthesis pathway of glycine betaine from the precursor choline, with glycine betaine aldehyde as the intermediate, has been elucidated by Boch *et al.*[17,20]

aldehyde dehydrogenase GbsA, with glycine betaine aldehyde as the intermediate (Fig. 1).[17]

Choline is an important component of lipids present in the eukaryotic cell membrane. Hydrolytic enzymes released by microorganisms can liberate the choline moiety from lipids of decaying cells; in soil environments, the primary source of choline is rotting plant material.[21,31] Since the choline content of the soil is very low and variable,[31] high-affinity uptake systems are required so that microorganisms can effectively scavenge it. The kinetic parameters of the osmotically inducible OpuB and OpuC transporters, with $K_m$ values in the low micromolar range and a substantial transport capacity, make these two ABC systems suitable for such a task.[24] Neither choline nor glycine betaine can be used as nutrients by *B. subtilis*.[21] Thus, they function exclusively as stress protectants, not only against osmotic stress[27] but also against high-temperature and low-temperature challenges.[32,33]

We report here the crystal structure of the OpuBC solute receptor in complex with its natural ligand, choline. The OpuBC/choline structure provides the molecular details of the architecture of the choline-binding site and a rational explanation as to why glycine betaine cannot be stably bound by the extracellular OpuBC substrate-binding protein.

## Results and Discussion

### Purification of the *B. subtilis* OpuBC protein

The OpuBC protein is initially synthesized as a precursor harboring a 22-amino-acid signal sequence to direct its export through the cytoplasmic membrane. During protein translocation, the OpuBC signal sequence is removed by a lipoprotein-specific signal sequence peptidase, and a lipid anchor is attached to the newly formed mature N-terminus (Cys23) to anchor it on the outer surface of the cytoplasmic membrane (Fig. 1).[24] We constructed an expression system for the *B. subtilis opuBC* gene that allowed the recombinant production of OpuBC in *E. coli* without the lipid anchor and its subsequent purification via Strep-tag II affinity chromatography (Fig. 2a).

### Substrate binding activity of OpuBC

The mature OpuBC protein contains 3 Trp residues and 17 Tyr residues spread throughout its sequence. We used intrinsic Trp/Tyr fluorescence to analyze the binding of choline to OpuBC (Fig. 2c). The addition of 100 μM choline led to an increase in the intensity of the intrinsic fluorescence (Fig. 2c),

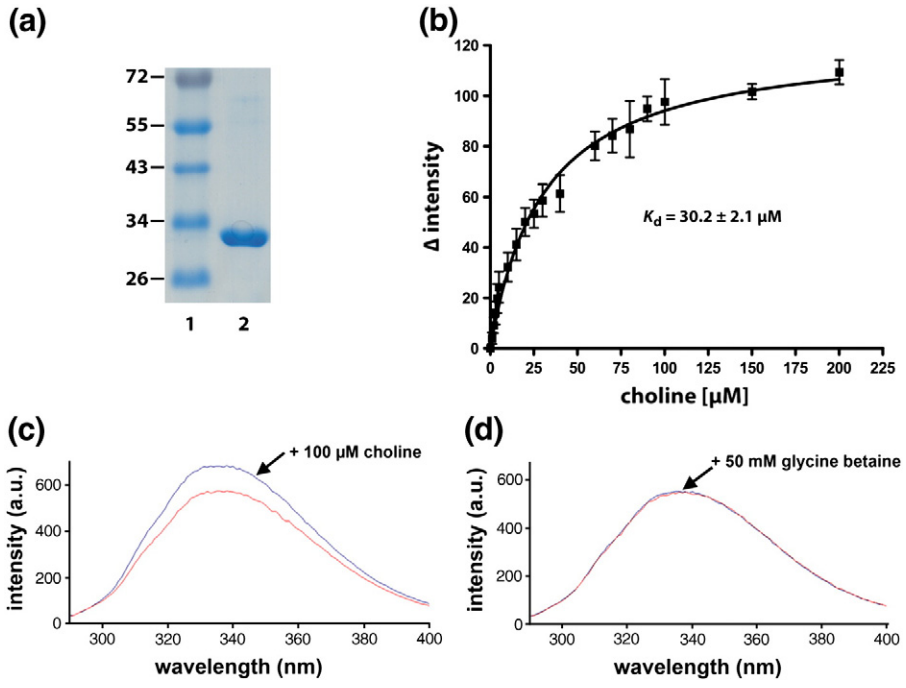


**Fig. 2.** Purified OpuBC protein and binding properties of the OpuBC/ligand complex. (a) A 12% SDS polyacrylamide gel of the purified OpuBC protein used for ligand binding and crystallization experiments; 5 μg of OpuBC protein was loaded on the gel. (b) Equilibrium binding titration experiments of OpuBC with choline. The dissociation constant of the OpuBC/choline complex was determined by intrinsic tyrosine and tryptophan fluorescence spectroscopy. For these experiments, the OpuBC concentration (1 μM) was kept constant, and the choline concentration was varied from 1 μM to 200 μM. (c) Emission spectra of OpuBC in the absence (red line) and in the presence (blue line) of 100 μM choline. (d) Emission spectra of OpuBC in the absence (red line) and in the presence (blue line) of 50 mM glycine betaine.

consistent with the expected binding of choline to OpuBC. In contrast, the addition of up to 50 mM glycine betaine did not change the fluorescence intensity (Fig. 2d). Since the properties of ligand-binding proteins typically determine the substrate specificity of a given microbial ABC importer,[34,35] the purified OpuBC exhibited a substrate specificity as expected from previously reported osmoprotection assays and transport experiments with osmotically stressed *B. subtilis* cells.[24]

### Equilibrium binding experiments of OpuBC with its ligand choline

The change in the intrinsic Trp/Tyr fluorescence of OpuBC observed after addition of choline (Fig. 2c) was used to determine the dissociation constant for the OpuBC/choline complex. For these experiments, we kept the OpuBC concentration constant (1 μM) and varied the choline concentration from 1 μM to 200 μM. The resulting spectroscopic data allowed us to calculated a $K_d$ value of 30.2 ± 2.1 μM (Fig. 2b). This $K_d$ value is very similar to that of the OpuAC/glycine betaine complex (approximately 20 μM).[36,37]

### The crystal structure of OpuBC from *B. subtilis* in complex with choline

As noted by Schiefner *et al.*, the amino acid sequence of OpuBC from *B. subtilis* is related (28% and 52% amino acid sequence identity and similarity, respectively) to the glycine-betaine-binding protein ProX from the hyperthermophilic archaeon *Archaeoglobus fulgidus*.[38] In particular, four Tyr residues that are part of the glycine betaine ligand-binding site of ProX[38] are conserved in the amino acid sequence of OpuBC (Fig. 3).

We solved the crystal structure of OpuBC in complex with choline. Crystals of OpuBC were grown in the presence of choline, and a native data set of the OpuBC/choline complex was collected at beamline ID-23 (European Synchrotron Radiation Facility, Grenoble, France) and scaled using XDS.[39] Initial phases were obtained by molecular replacement using the program Phaser,[40] with the crystal structure of ProX from *A. fulgidus* as template [Protein Data Bank (PDB) ID: 1SW2].[38] The final structure was refined to a resolution of 1.6 Å, which also allowed the modeling of water molecules. Data and refinement statistics, as well as model content, are summarized in Table 1.

The OpuBC/choline complex crystallized in a closed ligand-bound conformation. The overall structure is depicted in Fig. 4a and shows the typical bilobal fold of a solute receptor associated with microbial ABC-type importers.[34,35,43] OpuBC possesses two globular domains connected by two loops. A single choline molecule is trapped in a deep cleft formed by the two domains of OpuBC, a location of the ligand that is characteristic of

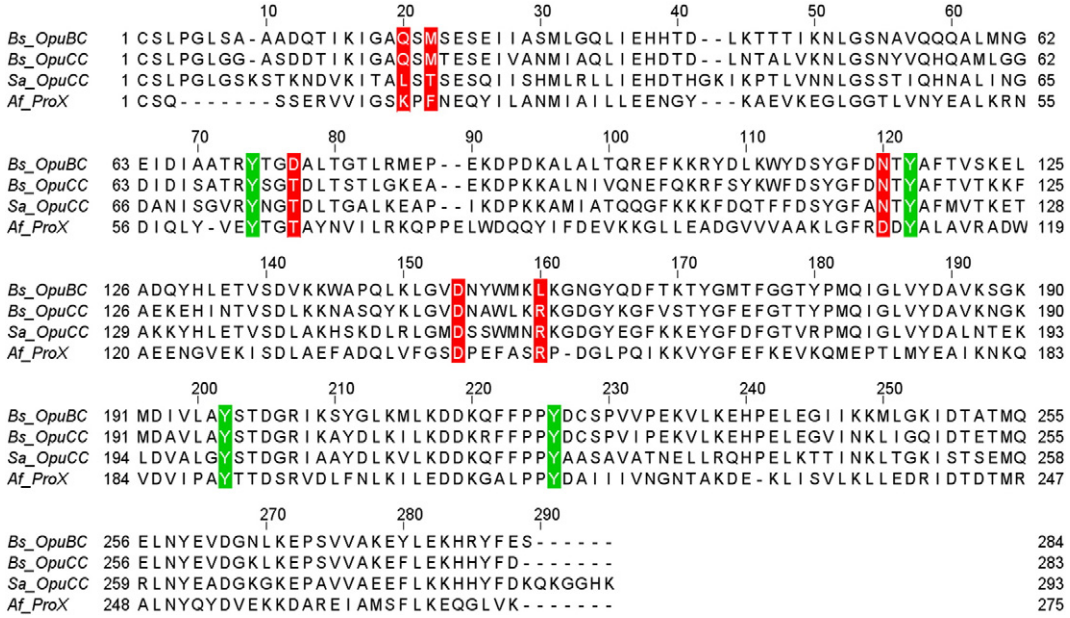


**Fig. 3.** Sequence alignment of OpuBC and OpuCC proteins from *B. subtilis*, ProX from *A. fulgidus*, and OpuCC from *St. aureus*. Shown is the alignment of the amino acid sequences (without the signal sequences) of the OpuBC and OpuCC proteins from *B. subtilis*, the ProX protein from *A. fulgidus*, and the OpuCC protein from *St. aureus*. Highlighted in green are amino acids forming the aromatic cage that bind the trimethyl ammonium head group of choline and glycine betaine. The amino acids binding the carboxyl group of glycine betaine and those that bind the alcohol group of choline are highlighted in red.

**Table 1.** Crystallographic parameters

| Space group | $P2_1$ |
|---|---|
| Unit cell parameters | |
| *a*, *b*, *c* (Å) | 29.7, 66.6, 63.8 |
| α, β, γ (°) | 90.0, 93.6, 90.0 |
| *Data collection and processing* | |
| Wavelength (Å) | 0.97625 |
| Resolution (Å) | 20–1.6 (1.7–1.6) |
| Mean redundancy | 1.86 (1.88) |
| Unique reflections | 30,684 |
| Completeness (%) | 93.1 (92.5) |
| $I/\delta$ | 12.1 (7.24) |
| $R_{sym}$ [a] | 6.0 (13.9) |
| *Refinement* | |
| $R_f$ [b] (%) | 16.6 (17.2) |
| $R_{free}$ [c] (%) | 20.6 (25.5) |
| RMSD from ideal | |
| Bond lengths (Å) | 0.007 |
| Bond angles (°) | 1.050 |
| Average *B*-factors (Å$^2$) | 10.20 |
| Protein | 13.02 |
| Ligand | 13.64 |
| Water | 24.78 |
| Ramachandran plot | |
| Most favored (%) | 98.2 |
| Allowed (%) | 1.8 |
| Disallowed (%) | 0.0 |
| Model content | |
| Monomers per asymmetric unit | 1 |
| Protein residues | 272 |
| Ligand | 1 |
| Water | 442 |

Crystal parameters and data collection statistics were derived from XDS. Refinement statistics were obtained from REFMAC5. Ramachandran analysis was performed using PROCHECK.[41,42]

[a] $R_{sym}$ is defined as $R_{sym} = \Sigma_{h\,kl}\,\Sigma_i\,|I_i(hkl) - \langle I(hkl)\rangle|\,/\,\Sigma_{h\,kl}\,\Sigma_i\,I_i(hkl)$.

[b] $R_f$ is defined as $R_f = \sum_{hkl}\,|F_{obs}| - |F_{calc}|\,/\,\sum_{hkl}\,|F_{obs}|$.

[c] $R_{free}$ is calculated as $R_f$, but for 5% randomly chosen reflections that were omitted from all refinement steps. Data in parentheses correspond to the highest-resolution shell.

substrate-binding proteins.[43] Domain I of the OpuBC protein comprises residues 4–107 and 213–275 (depicted in light blue), and domain II consists of residues 108–212 (depicted in light gray) (Fig. 4a). The two domains are formed by two central five-stranded β-sheets flanked by several α-helices. Residues 111–117 and 208–214 form the two hinge regions connecting these two domains. When one compares domain I with domain II of the OpuBC protein, it becomes apparent that the latter not only is smaller in size but also exhibits differences in secondary structure (Fig. 4a).

The *B. subtilis* OpuBC protein belongs to cluster F-III of the newly developed crystal-structure-based classification of substrate-binding proteins.[43] Cluster F contains solely class II substrate-binding proteins—solute receptors that possess two hinge regions connecting the two domains of the substrate-binding protein. A characteristic feature of the binding proteins grouped into cluster F-III is the presence of an extended-hinge segment that in all likelihood permits a more flexible domain movement between the substrate-free (open) conformation and the substrate-bound (closed) conformation.[43] In OpuBC, this extended-hinge segment comprises 10 residues and extends from Phe218 to Ser224. An additional but shorter hinge region spans from Asp113 to Tyr117 (Fig. 4a).

Although OpuBC and ProX proteins exhibit only a modest degree of amino acid sequence identity (28%) (Fig. 3), an overlay of the OpuBC/choline crystal complex with that of the ProX/glycine betaine crystal complex reveals a high degree of similarity (Fig. 5a) that is reflected in the 2.8-Å RMSD between both crystal structures for 206 $C^{\alpha}$ atoms. Thus, the overall fold of OpuBC from the mesophile *B. subtilis* (optimal growth temperature, 37 °C) and that of the ProX protein from the hyperthermophile *A. fulgidus* (optimal growth

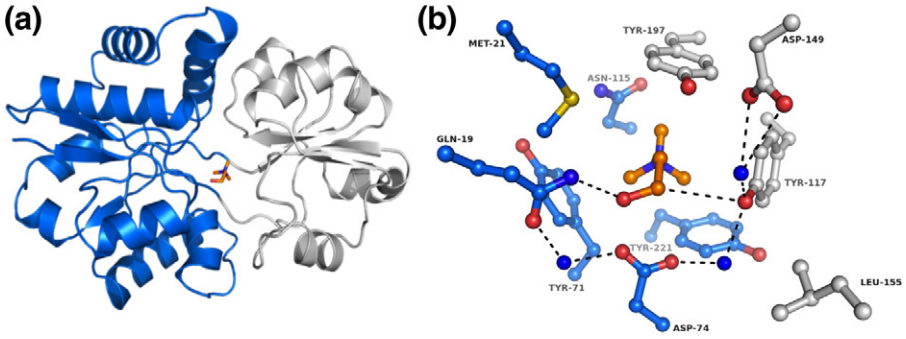


**Fig. 4.** Crystal structure of the OpuBC protein and its ligand-binding site. (a) Overall fold of the OpuBC protein from *B. subtilis*. The two-domain architecture of the OpuBC solute receptor is indicated in blue and light gray. Bound choline is represented as sticks. (b) Architecture of the ligand-binding pocket of the OpuBC protein with bound choline. Interactions of the hydroxyl tail of choline are highlighted with red broken lines. Both representations show the same orientation of the protein.

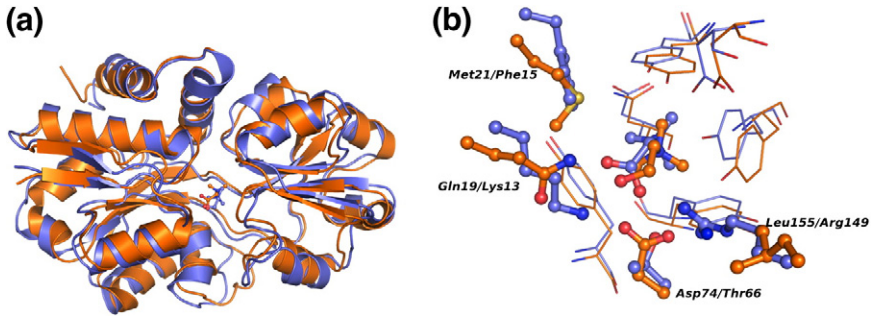


**Fig. 5.** Overlay of *B. subtilis* OpuBC and ProX from *A fulgidus*. (a) Residues belonging to the OpuBC protein (PDB ID: 3R6U) are shown in orange, and residues belonging to the ProX protein (PDB ID: 1SW2) are shown in light purple. (b) Architecture of the ligand-binding pocket of the OpuBC protein with bound choline and of the ProX protein with bound glycine betaine. The aromatic cages present in both proteins overlay perfectly and are shown as lines. Amino acids involved in the binding of the hydroxy/carboxy tail of the individual ligands are highlighted as stick representation.

temperature, 83 °C) are basically the same, with only a few minor exceptions in some of the outer loop regions (data not shown).

The substrate-binding proteins grouped into cluster F-III not only have a very similar overall structure but also possess ligand-binding sites with similar architectures.[43] The current functionally characterized members of cluster F-III are the glycine betaine/proline betaine-binding protein ProX from *E. coli*[44] and *A. fulgidus*,[38] the glycine betaine/proline betaine-binding protein OpuAC from *B. subtilis*[36,37] and *L. lactis*,[14] and the choline/acetylcholine-binding protein ChoX from *Sinorhizobium meliloti*.[45] The ligands of these solute receptors all possess bulky, positively charged trimethylammonium or dimethylammonium head groups. These are positioned within the ligand-binding site via cation–pi interactions,[46] with aromatic amino acid side chains forming a hydrophobic cage of varying geometries. As described below, the architecture of the substrate-binding site of OpuBC and the coordination of the choline ligand within the binding site confirm the features established for all members of cluster F-III of the structure-based binding protein classification scheme.[43]

## Architecture of the choline-binding site in OpuBC

The choline ligand is trapped deep in the cleft formed by the two lobes of the OpuBC protein (Fig. 4a). A closer inspection of the ligand-binding site revealed that residues originating from domains I and II (Fig. 4b) are used to shape the choline-binding site: side chains of Tyr71 and Tyr221 (domain I) and those of Tyr117 and Tyr197 (domain II) form an aromatic cage (Fig. 4b). This aromatic cage accommodates and coordinates the trimethylammonium moiety of choline. The positive charge of the head group of choline is not fixed on the nitrogen atom but delocalized over the three methyl groups of the ligand, thereby forming a bulky cation. The binding of this cation is established by interactions with the aromatic side chains of Tyr71, Tyr117, Tyr197, and Tyr221 via cation–pi interactions, as was previously found in ligand-binding proteins for various compatible solutes and osmoprotectants.[14,36–38,44,45] Distances between the carbon atom in the methyl groups of the choline head group and the four aromatic Tyr side chains are in the range of ~3.5 Å, consistent with their van der Waals radii. In addition to cation–pi interactions, the trimethylammonium group of choline interacts directly and is water mediated by Asp149. The hydroxyl tail of choline protrudes from the aromatic cage and possesses only one strong and direct interaction with Gln19, a residue that originates from domain I and has a distance of 2.7 Å to choline (Fig. 4b).

In addition to the ligand that interacts with residues originating from both domains, a domain–domain interaction that is mediated by a water molecule (water 127 according to PDB ID 3R6U, depicted as a blue sphere in Fig. 4b) is observed between Asp74 and Tyr117. This water-mediated interaction between the two lobes of OpuBC is further stabilized via the interactions of an additional water molecule with Leu155. Leu155 (located in domain II) interacts indirectly with Asp74 (located in domain I) via these two water molecules. Notably, these water-mediated interactions are—in addition to the interactions mediated by the trimethylammonium head group of choline—the only interactions present between domain I and domain II of OpuBC (Fig. 4b). In addition to these interactions, Asn115 appears to play an important role. Although not interacting with the substrate, this residue is near the binding site and is located inside the hinge region that connects the two lobes of the OpuBC protein (Fig. 4a). The side chain of Asn115 has interactions with both domains of OpuBC: Glu23 (domain I) and the backbone nitrogen of Ser198 (domain II). These interactions further stabilize the

closed choline-liganded conformation of OpuBC; a substitution of Asn115 with an Ala residue results in a loss of the binding of choline (see the text below).

## Mutational analysis of the choline-binding site in OpuBC

The aromatic cages that coordinate the head groups of choline in OpuBC and of glycine betaine in ProX[38] are superimposable (Fig. 5b). As a consequence of this arrangement, the trimethylammonium head groups of the choline and glycine betaine ligands are coordinated identically (Fig. 5b). The ProX protein from the hyperthermophile *A. fulgidus* binds its ligand glycine betaine with a $K_d$ of about 60 nM. The replacement of a single Tyr residue within the aromatic cage by Ala residues causes a drop in ligand binding affinity between 58-fold and 2500-fold, respectively, depending on which Tyr residue is mutated.[47] Hence, a mutant aromatic cage formed by only three Tyr residues still affords ligand binding by ProX with either good affinity or at least quite reasonable affinity. However, the simultaneous replacement of two Tyr residues by Ala residues (regardless of the combination) leads to a mutant ProX protein that is not capable of ligand binding.[47]

Since the aromatic cages present in the substrate-binding sites of ProX and OpuBC have identical architectures (Fig. 5b), we have not repeated a mutational analysis of the aromatic cage of the OpuBC protein. We surmise that the data obtained on ligand binding for ProX can be projected onto the ligand binding attributes of the OpuBC protein. Instead, we conducted a mutational analysis of the residue coordinating the hydroxyl moiety of choline and those residues that contribute to the domain–domain interactions of the two lobes of OpuBC and the buildup of the water network that stabilizes the ligand within the binding site. Therefore, we focused on Gln19, Asp74, Asp149, and Leu155. Each of these residues was separately replaced by an Ala residue, and each of the purified mutants was analyzed by intrinsic Trp/Tyr fluorescence.

Replacement of Gln19 by Ala reduced the binding affinity by about 14-fold (Table 2), highlighting the importance of the direct interaction of the Gln19 side chain with the hydroxyl group of choline for high-affinity ligand binding (Fig. 4b). However, those residues that are involved in setting up the water network within the ligand-binding site (Fig. 4b) were (at least) of equal importance as Gln19 for choline binding. The separate replacement of Asp149 and Leu155 with Ala residues led to an 18-fold drop and a 25-fold drop in ligand binding activity, with $K_d$ values of approximately 556 μM and 767 μM, respectively (Table 2). The simultaneous substitution of these two residues with Ala residues led to a $K_d$ of about 1 132 μM, a 38-fold drop in ligand binding affinity (Table 2). A key residue within the ligand-binding site is Asp74 (Fig. 4b). The side chain of Asp74 does not directly contact the ligand but triggers it via water-mediated interactions between Gln19 and Leu155, a stable domain closure of OpuBC. Consequently, it is critical for a stable entrapment of the ligand. Replacement of Asp74 by Ala generated an OpuBC variant that is unable to bind choline, even when the ligand is present at a concentration of 50 mM (Table 2). Likewise, the simultaneous replacement of Gln19 (which is in direct contact with choline) and Leu155 (a key residue for the formation of the water network) with Ala residues leads to a protein that no longer binds choline even at very high substrate concentrations (Table 2). Collectively, this mutational assessment of the ligand-binding site of OpuBC underscores the functional roles of those residues that were deduced from the crystal structure of OpuBC for both direct (Gln19) and water-mediated interactions (Asp74, Asp149, and Leu155) with choline and the two lobes of the protein.

**Table 2.** Mutation analysis of the choline-binding site of OpuBC

| Mutant | $K_d$ choline [μM] |
|---|---|
| Wild type | 30.5 ± 3.5 |
| Q19A | 434 ± 55 |
| M21A | 97 ± 14 |
| D74A | NB |
| N115A | NB |
| D149A | 556 ± 32 |
| L155A | 767 ± 77 |
| Q19A/L155A | 1450 ± 61 |
| D149A/L155A | 1132 ± 96 |

The affinities of the wild-type OpuBC protein and its mutant derivatives were assessed by intrinsic Trp/Tyr fluorescence. The data shown are the mean of three independent measurements. NB= no binding was observed under the experimental conditions used; the highest substrate concentration tested for these mutants was 50 mM.

It is generally thought that the interaction of the ligand with residues in the substrate-binding site induces a hinge-bending (and sometimes also a rotational motion) movement of the two domains of the binding protein. As a result, the substrate-binding site is dynamically formed with contributions from the residues of both domains of the binding protein. This hinge-bending motion leads to the entrapment of the ligand and the formation of the closed conformation of the binding protein. The hinge segments that connect the two lobes play a critical role for these domain movements.[43,45,48] Asn115 is part of one of the

two hinge segments (see the text above), and its replacement by Ala destroyed the ability of OpuBC to bind choline (Table 2). Hence, although Asn115 does not interact directly with the ligand, it strongly influences the substrate-induced closing of OpuBC via interaction with amino acids originating from both domain I and domain II (Glu23 and Ser198).

### Comparison of the choline-binding site of OpuBC with the glycine-betaine-binding site present in ProX from *A. fulgidus*

The architectures of the aromatic cages of OpuBC (Fig. 4b) and ProX[38] are identical (Fig. 5b). However, it has to be stressed that OpuBC does not bind glycine betaine (Fig. 2d) and that ProX does not bind choline.[47] These differences in ligand specificity are therefore caused by the different coordinations of the carboxylate group of glycine betaine and the hydroxyl group of choline, respectively.

The side chain of Gln19 plays an important role in the fixation of choline, since it interacts directly with the hydroxyl group of the ligand (Fig. 4b). At the equivalent position in ProX, a lysine residue (Lys13) that interacts directly with one of the two oxygens of the glycine betaine tail is present (Fig. 4b). The second oxygen of glycine betaine is coordinated through interactions with Arg149.[38] As described above, the interaction between both domains of OpuBC is mediated via a water network into which Leu155 is critically involved (Table 2). Strikingly, in a superimposition of the OpuBC and ProX crystal structures, a water molecule is located exactly at the position of the N3 atom of Arg149 of ProX (Fig. 5b). Hence, the strong interaction partners for the carboxylic tail of glycine betaine present in the ProX protein from *A. fulgidus* are absent in the OpuBC protein from *B. subtilis*. As a result, glycine betaine cannot be bound stably despite the fact that its trimethylammonium head group would fit correctly into the aromatic Tyr cage of the OpuBC protein (Figs. 4b and 5b).

Our analysis of the crystal structures of OpuBC and ProX therefore suggests that glycine betaine is unable to induce a closure of the two domains of OpuBC, thereby forming the stable closed conformation of the solute receptor. This closed conformation, however, is required for productive interactions of the substrate-loaded binding proteins with the membrane-embedded components of the cognate ABC transport system.[49,50] Hence, the crystal structure of the OpuBC protein in complex with its natural ligand choline provides a rational for the observed choline specificity of the OpuB ABC importer *in vivo*[24] and its inability to catalyze the import of glycine betaine.[23]

### Analysis of the crystal structure of OpuCC from *Staphylococcus aureus*, a ligand-binding protein related to the OpuBC and OpuCC proteins from *B. subtilis*

In the Brookhaven Protein Databank‡, a crystal structure of an OpuCC protein from a *St. aureus* strain has been deposited (PDB ID: 3O66), but the features of the OpuCC-3O66 protein have not been published. OpuCC-3O66 is annotated in the PDB as a glycine betaine/carnitine/choline-binding protein, but no functional data are available to assess its substrate specificity. However, a sequence-related OpuCC protein from the *St. aureus* strain RN6390 is part of a functionally characterized ABC importer for choline.[51] Due to the high degree of the amino acid sequence relatedness of OpuCC-3O66 with the *B. subtilis* OpuBC (56% identity and 73% homology) and OpuCC (59% identity and 76% homology) proteins (Fig. 3), we compared the crystal structures of OpuCC-3O66 and OpuBC. The superimposition of these two crystal structures (Fig. 6a) revealed that the OpuCC-3O66 protein has been crystallized in an open unliganded conformation. This open conformation is stabilized by two triethylene glycol molecules bound between both domains of OpuCC-3O66, a position where the ligand is expected to be localized.[43,48] By structural alignment, the domain closure upon substrate binding can be visualized for these two proteins (Fig. 6b). We used domain II as an anchor point, and the residues originating from this domain align nicely between the OpuBC structure and the OpuCC-3O66 structure. Interestingly, also the tyrosine residues of domain I are only slightly differently orientated in the binding site when one compares the closed OpuBC structure with that of the open OpuCC-3O66 structure (Fig. 6b). This suggests that the Tyr cage of the binding site is already prearranged in the open conformation of the OpuCC-3O66 protein and indicates that only small conformational changes have to occur upon binding of the substrates to lead to the closed conformation of the binding protein. In contrast, the other amino acids of the OpuCC-3O66 protein must go through a larger movement. Especially Leu40 in the OpuCC-3O66 structure appears to undergo a large conformational change, since it should be located on the position of Gln19 in the closed OpuBC structure. Also Thr97 of the OpuCC-3O66 protein should be mentioned here, since it is likely a key residue for domain closure; its counterpart in OpuBC would be Asp74 (Fig. 6b). This Asp74 residue is likely responsible for the narrow substrate specificity of OpuBC for choline. Replacement of this amino acid may alter substrate specificity for other substrates, like in the case of

‡ www.pdb.org

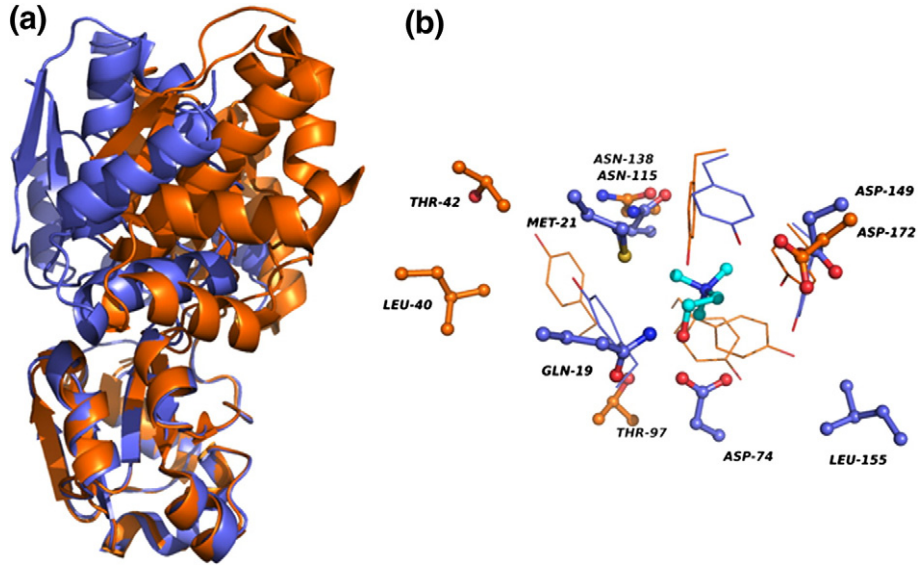


**Fig. 6.** Superimposition of the crystal structures of the OpuBC protein from *B. subtilis* and the OpuCC protein from *S. aureus*. (a) Overlay of the OpuBC and OpuCC proteins. OpuBC is shown in blue, and OpuCC is depicted in orange. (b) Overlay of OpuBC-binding site with residues of OpuCC that align in Fig. 3. The residues of domain II of both proteins overlap well, whereas an outward rotation of domain I of the OpuCC protein, in comparison to the OpuBC protein, indicates an open ligand-free conformation of the *St. aureus* OpuCC protein (PDB ID: 3O66).

Thr97 in OpuCC. However, it is also likely that the affinity in such a mutated binding site drops.

### Comparison of the ligand-binding site in OpuBC with the choline-binding site of ChoX from *S. meliloti*

In addition to the *B. subtilis* OpuBC/choline crystal structure described here, only one further crystal structure of a substrate-binding protein that is specific for choline and associated with an ABC transporter has been reported.[45] The ChoX protein has been crystallized in the choline-bound and acetylcholine-bound closed conformation, in a semi-open conformation without a ligand, and in a fully closed but substrate-free conformation.[45,52] An overlay of the crystal structures of the OpuBC and ChoX proteins in complex with their common ligand choline is depicted in Fig. 7a. The similarity of these two structures is reflected by an RMSD of 2.1 Å for 213 $C^{\alpha}$ atoms, although the amino acid sequence of the OpuBC and ChoX proteins is only moderately related (25% identity and 50% homology).

Despite the fact that the overall structures of both proteins are similar, the details of the architecture of the choline-binding site differ substantially between OpuBC and ChoX (Fig. 7b). Three Trp residues and one Tyr residue form the aromatic cage of the ligand-binding site of ChoX, whereas four Tyr residues form the aromatic cage in OpuBC. The hydroxyl group of choline is bound via an interaction with the ND2 atom of Asn156 in ChoX; this is similar to the configuration observed in OpuBC, where the hydroxyl function of choline interacts with Gln19 (Fig. 4b). Compared to OpuBC ($K_d = 30.2 \pm 2.1$ μM) (Table 2), ChoX exhibits a

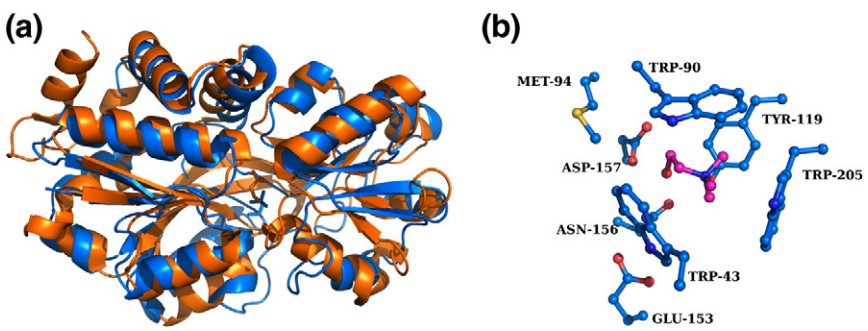


**Fig. 7.** Superimposition of the crystal structures of the OpuBC protein from *B. subtilis* and the ChoX protein from *S. meliloti*. (a) Overlay of the OpuBC and ChoX proteins. OpuBC is shown in orange, and ChoX is depicted in light blue. (b) View of the binding site of ChoX. For clarity, no overlay with the OpuBC choline-binding site is shown, since the choline-binding site present in ChoX is not superimposable with that of OpuBC in the structural alignment.

somewhat higher affinity for its ligand choline ($K_d = 2.3 \pm 1$ μM).[45,53] These differences in affinity can probably be attributed to the stronger cation–pi interactions mediated by the aromatic side chains of Trp residues in comparison to those mediated by Tyr residues.[46]

### The OpuBC crystal structure as a functional and structural template for a large family of microbial substrate-binding proteins

We conducted a BLAST search[54] in microorganisms with completely sequenced genomes (1497 entries) for proteins related to the amino acid sequence of OpuBC. We recorded well over a thousand hits, indicating that OpuBC-related proteins are represented widely in the microbial world. Eleven OpuBC-related proteins were found in the Euryarchaeota subtree of the domain of Archaea to which *A. fulgidus* belongs. Each of these proteins was associated with an ABC transport system, as judged from the inspection of the genome context of the corresponding *opuBC*-related structural genes using the gene neighborhood tool provided by the Joint Genome Institute (JGI) Web server. The four Tyr residues forming the aromatic cages in the *B. subtilis* OpuBC protein (Fig. 4b) and the *A. fulgidus* ProX protein (Fig. 5b) are either conserved or conservatively substituted, suggesting that each of these substrate-binding proteins is involved in capturing ligands with fully methylated nitrogens (e.g., glycine betaine, choline, choline-*O*-sulfate, carnitine, and proline betaine) or sulfonium head groups (e.g., dimethylsulfonioacetate).[36] In addition to OpuBC-related binding proteins that were associated with ABC transporters in members of Archaea, our database search also detected an OpuBC-related protein with a conserved aromatic cage, CosB, in the extreme halophilic archaeon *Halobacterium salinarum*. Interestingly, the CosB ligand-binding protein is not associated with the functioning of an ABC transporter. Instead, it is part of an intriguing sensory transduction system that allows *H. salinarum* to conduct chemotaxis towards the osmoprotectants glycine betaine, carnitine, and choline.[55]

OpuBC-related proteins are prevalent in members of the domain of Bacteria. We aligned the amino acid sequences of 1000 OpuBC-type proteins using the CLUSTAL W algorithm[56] and found that the four Tyr residues forming the aromatic cage were either fully conserved or conservatively substituted; there are very few exceptions where only three aromatic residues are present (data not shown). Hence, it is likely that aromatic cages of the type present in OpuBC and ProX are also present in all these proteins. In view of the data available from the crystal structures and mutational analysis of *A. fulgidus* ProX[38,47] and *B. subtilis* OpuBC (this study), we consider it highly likely that the predicted aromatic cages of these 1000 solute receptors will participate in ligand binding. Although most of the 1000 OpuBC-related proteins that we inspected are annotated in the National Center for Biotechnology Information Institute database as substrate-binding proteins with a putative substrate specificity for choline, glycine betaine, or carnitine, the *in silico* predictions of specific ligands for these proteins in database entries should be viewed with some caution. However, a careful inspection of those residues forming the ligand-binding sites in the crystal structures of the choline-specific OpuBC protein from *B. subtilis* (this study) and its OpuCC counterpart with a broader substrate specificity are likely to give experimentally testable clues for assessing the ligand-binding profile of individual members of the OpuBC/OpuCC/ProX family of substrate-binding proteins.

## Conclusions

The OpuBC crystal structure, in conjunction with site-directed mutagenesis, revealed the molecular basis for high-affinity choline binding by the cell-surface-exposed OpuBC solute receptor of *B. subtilis*. Furthermore, a careful analysis of the OpuBC/choline complex and a structure-guided comparison with the architecture of the ligand-binding site present in ProX from the hyperthermophilic archaeon *A. fulgidus* also provide a rational explanation as to why glycine betaine, a substrate for the OpuC transporter but not for the OpuB system (Fig. 1), cannot be stably bound by OpuBC. The structural and functional analyses of OpuBC highlight a new binding site for choline with remarkable similarities to, but also functionally important differences from, the glycine-betaine-binding site. Furthermore, our data suggest that binding sites for the same ligand (e.g., choline) can still vary between organisms, as revealed here, through the comparison of the ChoX and OpuBC choline-binding proteins.

## Materials and Methods

### Chemicals

Choline, glycine betaine, anhydrotetracyline, 2-[4′-hydroxy-benzeneazo] benzoic acid, and desthiobiotin were purchased from Sigma-Aldrich (Munich, Germany). Ampicillin was purchased from Carl Roth (Karlsruhe, Germany), and gentamicin was obtained from Serva (Heidelberg, Germany). The matrices (*Strep*-Tactin Sepharose) for the affinity purification of recombinant proteins marked with Strep-tag II were purchased from IBA (Göttingen, Germany).

### Bacterial strains and growth media

Chromosomal DNA of the *B. subtilis* wild-type strain JH642 (*trpC pheA1*; BGSC 1A96; a kind gift of J. Hoch, Scripps Research Institute, La Jolla, CA, USA) was used as donor for the cloning of the *opuBC* gene. Strain JH642 was propagated aerobically in Luria–Bertani liquid medium at 37 °C.[57] The *E. coli* strain DH5α (Fermentas, St. Leon-Rot, Germany) was used for all cloning experiments. For the overproduction of recombinant OpuBC and its mutants, we used the *E. coli* strain BL21 [Artic express (DE) RIL] (Stratagene, La Jolla, CA, USA). Overproduction of OpuBC and its derivatives was carried out in a slightly modified minimal medium (MMA)[57] supplemented with 1 mg/L thiamine, 1 mM $MgSO_4$, 0.2% casamino acids (wt/vol), 0.5% glucose (wt/vol) as carbon source, and 100 μg/ml ampicillin to select for recombinant plasmids carrying the *opuBC* gene or its mutant derivatives.

### Cloning and site-directed mutagenesis of the *B. subtilis opuBC* gene

The coding region of *opuBC* was cloned without the signal sequence, and the codon for Cys23 was replaced by a codon encoding a Gly residue. PCR was carried out with the forward (5′-CGTCTCCGCGCGGCTCGCTTCCTGGTCTCAGCGC-3′) and backward (5′-CGTCTCGTATCTCACGATTCGAAATAGCGATGTTTTTC-3′) primers on chromosomal DNA isolated from the *B. subtilis* wild-type strain JH642. The resulting 877-bp *opuBC* DNA fragment was cleaved with Esp3I (recognition sequences for Esp3I in the primer sequence are underlined) and then cloned into the expression vector pASK-IBA6 (IBA) that had been cut with BsaI. The DNA sequence of one of the resulting plasmids, pMP31, was determined (Eurofins MWG Operon, Ebersberg, Germany) to ensure that no mutations had been introduced into the *opuBC* coding sequence during the cloning procedure. In plasmid pMP31, the coding region of *opuBC* is inserted into the pASK-IBA6 vector in such a way that it is fused to an OmpA signal sequence for export from the *E. coli* cell, followed by the Strep-tag II affinity peptide and a cleavage site for Factor Xa protease. Expression of the hybrid *opuBC* gene in plasmid pMP31 is under the control of the anhydrotetracycline-responsive TetR repressor that is encoded by the pASK-IBA6 expression vector.

Mutant derivatives of the *opuBC* gene were generated with the QuickChange site-directed mutagenesis kit (Stratagene) using plasmid pMP31 as DNA template and custom-synthesized mutagenic DNA primers (purchased from Sigma-Aldrich). The following mutant *opuBC* plasmids were created: pMP49 [Gln19→Ala (CAA/GCA)], pMP51 [Asp74→Ala (GAC/GCC)], pMP52 [Asn115→Ala (AAT/GCT)], pMP53 [Leu155→Ala (CTC/GCC)], and pMP65 [Asp149→Ala (GAT/GCT)]. Selected mutant plasmids with single amino acid substitutions in the OpuBC protein were remutagenized to generate the following double *opuBC* mutant derivatives: pMP62 [Gln19→Ala (CAA/GCA) and Leu155→Ala (CTC/GCC)] and pMP66 [Asp149→Ala (GAT/GCT) and Leu155→Ala (CTC/GCC)]. The entire coding region of each of the mutant *opuBC* alleles was sequenced to ensure the presence of the desired mutation and the absence of unwanted DNA alterations.

### Overexpression and purification of recombinant OpuBC proteins in *E. coli*

Plasmid pMP31 (resistant to ampicillin) was transformed into competent cells of the *E. coli* strain BL21 [Artic express (DE) RIL] (resistant to gentamicin) by simultaneously selecting for ampicillin-resistant (100 μg/ml) and gentamicin-resistant (20 μg/ml) transformants on LB agar plates. One of the antibiotic-resistant colonies was then picked and used to inoculate a preculture (100 ml of modified MMA containing the antibiotics ampicillin and gentamicin at the above indicated concentrations) that was then propagated overnight at 37 °C in a 1-L Erlenmeyer flask in an aerial shaker set at 200 rpm. For the main culture, we used a Minifors fermenter system (Infors AG, Bottmingen, Switzerland) with a 5-L reaction vessel filled with 4 L of modified MMA (see above) containing 100 μg/ml ampicillin. The medium present in the fermenter vessel was inoculated with the preculture of strain BL21 [Artic express (DE) RIL] (pMP31) to an $OD_{578}$ of about 0.1. The cells were then grown at 37 °C first as batch culture (up to an $OD_{578}$ of about 3) and subsequently as a fed-batch culture up to an $OD_{578}$ of about 15. Then, the temperature of the culture was cooled to 20 °C, and the expression of the TetR-controlled *opuBC* gene present in plasmid pMP31 was induced by the addition of anhydrotetracycline (0.2 mg anhydrotetracyline/L/$OD_{578}$ = 1) to the culture. The bacterial cells were then propagated under *opuBC*-inducing conditions for an additional 16 h at 20 °C and were subsequently harvested by centrifugation (30 min, 3000*g*, 4 °C). The cells (10 g wet weight) were resuspended in 20 ml of buffer W [100 mM Tris–HCl (pH 7.5) and 150 mM NaCl] and disrupted by passing them five times through a French pressure cell (1000 psi) at 4 °C. Unbroken cells and cellular debris were removed by centrifugation (1 h, 35,000*g*, 4 °C), and the supernatant was loaded onto a 10-ml *Strep*-Tactin column (IMA, Göttingen, Germany) preequilibrated with 10 column volumes of buffer W [100 mM Tris–HCl (pH 7.5) and 150 mM NaCl]. After the column had been washed with 20 column volumes of buffer W, proteins bound to the affinity matrix were eluted with 3 column volumes of buffer E [100 mM Tris–HCl (pH 7.5) and 150 mM NaCl] containing 2.5 mM desthiobiotin. OpuBC-containing fractions were collected in 3-ml portions, the protein concentration was estimated with a NanoDrop spectrometer (Thermo Scientific, Wilmington, DE, USA), and the purity of the OpuBC protein was assessed by SDS gel electrophoresis. Two forms of the recombinantly produced OpuBC protein were found: (i) the nonprocessed OmpA Strep-tag II OpuBC protein and (ii) the processed Strep-tagII OpuBC protein.

All fractions containing OpuBC proteins were pooled and concentrated using Vivaspin 4 concentrator columns (exclusion size, 10 kDa) (Vivascience, Hannover, Germany) with a simultaneous exchange of the buffer with 10 mM Tris–HCl (pH 7.5) and 10 mM NaCl. The nonprocessed OmpA Strep-tag II and the processed Strep-tag II portions of the OpuBC protein were then treated with Factor Xa (Merck, Darmstadt, Germany) to remove the OmpA signal sequence and the Strep-tag II affinity peptide. Proteolytic cleavage of the recombinant OpuBC protein with Factor Xa was carried out at room temperature overnight (0.5 U/50 μg of OpuBC protein in the cleavage buffer provided by Merck). The completeness

of the proteolytic cleavage of the two forms of the recombinant OpuBC protein was assessed by SDS gel electrophoresis and found to yield a single OpuBC band on a 12% SDS polyacrylamide gel (Fig. 2a). The OpuBC protein was then applied to a 5-ml ion-exchange column (HiTrap QFF 5; GE Healthcare, Munich, Germany) equilibrated with 2 column volumes of buffer A [25 mM Tris–HCl (pH 7.5) and 20 mM NaCl]. Functional OpuBC protein (as assessed by fluorescence spectroscopy) was eluted from the HiTrap QFF 5 column by applying a gradient of buffer B [25 mM Tris–HCl (pH 7.5) and 1000 mM NaCl]. From a typical overproduction (from 4 L of culture) and purification experiment, we obtained approximately 20 mg of pure and active protein. For crystallization trials and ligand binding experiments, the purified OpuBC protein was concentrated to about 10 mg/ml with Vivaspin 4 concentrator columns (exclusion size, 10 kDa) (Vivascience), with a simultaneous exchange of the buffer with 10 mM Tris–HCl (pH 7.5) and 10 mM NaCl. All mutant derivatives of OpuBC were overproduced and purified as described above for the wild-type protein.

### Determination of the dissociation constant of the OpuBC/choline complex

The dissociation constant of the OpuBC/choline complex was determined by intrinsic tyrosine and tryptophan fluorescence spectroscopy, as described for the glycine-betaine-binding protein OpuAC from *B. subtilis*.[36,37] OpuBC possesses 3 Trp residues and 17 Tyr residues, and the intrinsic fluorescence of these residues was monitored from 290 nm to 400 nm by using a Cary Eclipse fluorescence spectrometer (Varian, Surry, UK). The excitation wavelength was set to 285 nm, the slit width was 5 nm, the emission wavelength was 335 nm, and the temperature during the assays was maintained at 25 ± 1 °C with a cooling/heating device. One-milliliter samples of 1 μM OpuBC protein (in 10 mM Tris–HCl, pH 7.5) were equilibrated for 15 min in the cuvette. Subsequently, different amounts of choline (1–200 μM) were titrated to the protein solution, and fluorescence was recorded. Upon choline binding, an increase in fluorescence intensity was detected (Fig. 2b), and this change in the emission spectrum was used to determine the apparent $K_d$ value of OpuBC for choline by plotting the change in fluorescence intensity at 335 nm against the choline concentration. All given $K_d$ values of the wild-type OpuBC protein and its mutant derivatives (Table 2) represent the average of three independent measurements, with standard deviations given as errors.

### Crystallization of the OpuBC/choline complex, data collection, and model refinement

Crystals of OpuBC were obtained using the hanging-drop vapor diffusion technique at 12 °C. Purified OpuBC was concentrated to 10 mg/ml and incubated with 15 mM choline chloride prior to crystallization. One microliter of protein was mixed with 1 μl of reservoir solution containing 200 mM potassium acetate and 20% polyethylene glycol 3350. Crystals appeared after 3 days; were harvested after 2 weeks in 200 mM potassium acetate, 20% polyethylene glycol 3350, and 30% ethylene glycol; and flash frozen in liquid nitrogen.

A native data set of the OpuBC/choline complex was collected at beamline ID23-eh1 (European Synchrotron Radiation Facility) and scaled using XDS.[39] Initial phases were obtained by molecular replacement using the program Phaser,[40] with the crystal structure of *A. fulgidus* glycine-betaine-binding protein ProX used as template (PDB ID: 1SW2).[38] Data refinement statistics and model content are summarized in Table 1. Model building and refinement were performed using Coot and REFMAC5.[58]

### Database searches and computer analysis of protein sequences

Proteins that are homologous to OpuBC from *B. subtilis* were searched via the Web server of the DOI JGI§ or that of the National Center for Biotechnology Information Institute‖ using the BLAST algorithm.[54] The genome context of finished and unfinished microbial genomes in the vicinity of *opuBC*-type genes was assessed using the gene neighborhood tool¶ provided by the JGI Web server. Amino acid sequence alignments of proteins related to OpuBC were performed with CLUSTAL W.[56]

### Structure alignments

Structure alignments were performed using LSQMAN employing standard settings.

### Figure preparation

Figures of protein structures were prepared using PyMOL[a].

### PDB accession number

The coordinates and structure factors for the OpuBC/choline complex have been deposited in the PDB, Research Collaboratory for Structural Bioinformatics, Rutgers University (New Brunswick, NJ, USA), under accession code 3R6U[b].

## Acknowledgements

We thank the members of the laboratory of L.S. and E.B. for stimulating discussions, and Dr. Paul Tucker and Dr. Matthew Groves at the BW7A beamline, European Molecular Biology Laboratory outstation (Hamburg, Germany), for help with

§ http://www.jgi.doe.gov/
‖ http://www.ncbi.nlm.nih.gov/
¶ http://img.jgi.doe.gov/cgi-bin/pub/main.cgi/
[a] http://pymoil.sourcegorge.net/
[b] www.rcsb.org

the initial screening of the OpuBC crystals. Especially, we would like to thank Christoph Müller-Dieckmann of European Molecular Biology Laboratory outstation (Grenoble, France) for his continued support and expert advice during data collection and refinement. We appreciate the expert technical assistance of Jochen Sohn, and we are grateful to Vickie Koogle for her kind help in editing the manuscript.

Financial support for this study was provided by the LOEWE program of the State of Hessen (via the Center for Synthetic Microbiology; SynMicro, Marburg, Germany) and the Fonds der Chemischen Industrie (to E.B.). B.T. and L.S. gratefully acknowledge financial support by the EDICT EU-Program.

## References

1. Kempf, B. & Bremer, E. (1998). Uptake and synthesis of compatible solutes as microbial stress responses to high osmolality environments. *Arch. Microbiol.* **170**, 319–330.
2. Wood, J. M., Bremer, E., Csonka, L. N., Kraemer, R., Poolman, B., van der Heide, T. & Smith, L. T. (2001). Osmosensing and osmoregulatory compatible solute accumulation by bacteria. *Comp. Biochem. Physiol. Part A*, **130**, 437–460.
3. Bremer, E. & Krämer, R. (2000). Coping with osmotic challenges: osmoregulation through accumulation and release of compatible solutes. In *Bacterial Stress Responses* (Storz, G. & Hengge-Aronis, R., eds), pp. 79–97, ASM Press, Washington, DC.
4. Wood, J. M. (2011). Osmotic stress. In *Bacterial Stress Responses* (Storz, G. & Hengge, R., eds), pp. 133–156, ASM Press, Washington, DC.
5. Cayley, S. & Record, M. T., Jr (2003). Roles of cytoplasmic osmolytes, water, and crowding in the response of *Escherichia coli* to osmotic stress: biophysical basis of osmoprotection by glycine betaine. *Biochemistry*, **42**, 12596–12609.
6. Burg, M. B. & Ferraris, J. D. (2008). Intracellular organic osmolytes: function and regulation. *J. Biol. Chem.* **283**, 7309–7313.
7. Yancey, P. H. (2005). Organic osmolytes as compatible, metabolic and counteracting cytoprotectants in high osmolarity and other stresses. *J. Exp. Biol.* **208**, 2819–2830.
8. Le Rudulier, D., Strom, A. R., Dandekar, A. M., Smith, L. T. & Valentine, R. C. (1984). Molecular biology of osmoregulation. *Science*, **224**, 1064–1068.
9. Ziegler, C., Bremer, E. & Krämer, R. (2010). The BCCT family of carriers: from physiology to crystal structure. *Mol. Microbiol.* **78**, 13–34.
10. Poolman, B., Spitzer, J. J. & Wood, J. M. (2004). Bacterial osmosensing: roles of membrane structure and electrostatics in lipid–protein and protein–protein interactions. *Biochim. Biophys. Acta*, **1666**, 88–104.
11. Ressl, S., Terwisscha van Scheltinga, A. C., Vonrhein, C., Ott, V. & Ziegler, C. (2009). Molecular basis of transport and regulation in the Na(+)/betaine symporter BetP. *Nature*, **458**, 47–52.
12. Perez, C., Koshy, C., Ressl, S., Nicklisch, S., Krämer, R. & Ziegler, C. (2011). Substrate specificity and ion coupling in the Na(+)/betaine symporter BetP. *EMBO J.* **30**, 1221–1229.
13. Mahmood, N. A., Biemans-Oldehinkel, E. & Poolman, B. (2009). Engineering of ion sensing by the cystathionine beta-synthase module of the ABC transporter OpuA. *J. Biol. Chem.* **284**, 14368–14376.
14. Wolters, J. C., Berntsson, R. P., Gul, N., Karasawa, A., Thunnissen, A. M., Slotboom, D. J. & Poolman, B. (2010). Ligand binding and crystal structures of the substrate-binding domain of the ABC transporter OpuA. *PLoS One*, **5**, e10361.
15. Keates, R. A., Culham, D. E., Vernikovska, Y. I., Zuiani, A. J., Boggs, J. M. & Wood, J. M. (2010). Transmembrane helix I and periplasmic loop 1 of *Escherichia coli* ProP are involved in osmosensing and osmoprotectant transport. *Biochemistry*, **49**, 8847–8856.
16. Nyyssölä, A., Kerovuo, J., Kaukinen, P., von Weymarn, N. & Reinikainen, T. (2000). Extreme halophiles synthesize betaine from glycine by methylation. *J. Biol. Chem.* **275**, 22196–22201.
17. Boch, J., Kempf, B., Schmid, R. & Bremer, E. (1996). Synthesis of the osmoprotectant glycine betaine in *Bacillus subtilis*: characterization of the *gbsAB* genes. *J. Bacteriol.* **178**, 5121–5129.
18. Rosenstein, R., Futter-Bryniok, D. & Götz, F. (1999). The choline-converting pathway in *Staphylococcus xylosus* C2A: genetic and physiological characterization. *J. Bacteriol.* **181**, 2273–2278.
19. Lamark, T., Kaasen, I., Eshoo, M. W., Falkenberg, P., McDougall, J. & Strom, A. R. (1991). DNA sequence and analysis of the *bet* genes encoding the osmoregulatory choline–glycine betaine pathway of *Escherichia coli*. *Mol. Microbiol.* **5**, 1049–1064.
20. Finnegan, S., Yuan, H., Wang, Y. F., Orville, A. M., Weber, I. T. & Gadda, G. (2010). Structural and kinetic studies on the Ser101Ala variant of choline oxidase: catalysis by compromise. *Arch. Biochem. Biophys.* **501**, 207–213.
21. Boch, J., Kempf, B. & Bremer, E. (1994). Osmoregulation in *Bacillus subtilis*: synthesis of the osmoprotectant glycine betaine from exogenously provided choline. *J. Bacteriol.* **176**, 5364–5371.
22. Kempf, B. & Bremer, E. (1995). OpuA, an osmotically regulated binding protein-dependent transport system for the osmoprotectant glycine betaine in *Bacillus subtilis*. *J. Biol. Chem.* **270**, 16701–16713.
23. Kappes, R. M., Kempf, B. & Bremer, E. (1996). Three transport systems for the osmoprotectant glycine betaine operate in *Bacillus subtilis*: characterization of OpuD. *J. Bacteriol.* **178**, 5071–5079.
24. Kappes, R. M., Kempf, B., Kneip, S., Boch, J., Gade, J., Meier-Wagner, J. & Bremer, E. (1999). Two evolutionarily closely related ABC-transporters mediate the uptake of choline for synthesis of the osmoprotectant glycine betaine in *Bacillus subtilis*. *Mol. Microbiol.* **32**, 203–216.
25. Hahne, H., Mäder, U., Otto, A., Bonn, F., Steil, L., Bremer, E. *et al.* (2010). A comprehensive proteomics and transcriptomics analysis of *Bacillus subtilis* salt stress adaptation. *J. Bacteriol.* **192**, 870–882.
26. Steil, L., Hoffmann, T., Budde, I., Völker, U. & Bremer, E. (2003). Genome-wide transcriptional profiling

analysis of adaptation of *Bacillus subtilis* to high salinity. *J. Bacteriol.* **185**, 6358–6370.
27. Bremer, E. (2002). Adaptation to changing osmolarity. In *Bacillus subtilis and Its Closest Relatives* (Sonenshein, A. L., Hoch, J. A. & Losick, R., eds), pp. 385–391, ASM Press, Washington, DC.
28. Nau-Wagner, G., Boch, J., Le Good, J. A. & Bremer, E. (1999). High-affinity transport of choline-*O*-sulfate and its use as a compatible solute in *Bacillus subtilis*. *Appl. Environ. Microbiol.* **65**, 560–568.
29. Kappes, R. & Bremer, E. (1998). Response of *Bacillus subtilis* to high osmolarity: uptake of carnitine, crotonobetaine and γ-butyrobetaine via the ABC transport system OpuC. *Microbiology*, **144**, 83–90.
30. Jebbar, M., von Blohn, C. & Bremer, E. (1997). Ectoine functions as an osmoprotectant in *Bacillus subtilis* and is accumulated via the ABC-transport system OpuC. *FEMS Microbiol. Lett.* **154**, 325–330.
31. Kortstee, G. J. J. (1970). The aerobic decomposition of choline by microorganisms. *Arch. Microbiol.* **71**, 235–244.
32. Holtmann, G. & Bremer, E. (2004). Thermoprotection of *Bacillus subtilis* by exogenously provided glycine betaine and structurally related compatible solutes: involvement of Opu transporters. *J. Bacteriol.* **186**, 1683–1693.
33. Hoffmann, T. & Bremer, E. (2011). Protection of *Bacillus subtilis* against cold stress via compatible-solute acquisition. *J. Bacteriol.* **193**, 1552–1562.
34. Eitinger, T., Rodionov, D. A., Grote, M. & Schneider, E. (2011). Canonical and ECF-type ATP-binding cassette importers in prokaryotes: diversity in modular organization and cellular functions. *FEMS Microbiol. Rev.* **35**, 3–67.
35. Davidson, A. L., Dassa, E., Orelle, C. & Chen, J. (2008). Structure, function, and evolution of bacterial ATP-binding cassette systems. *Microbiol. Mol. Biol. Rev.* **72**, 317–364.
36. Smits, S. H., Höing, M., Lecher, J., Jebbar, M., Schmitt, L. & Bremer, E. (2008). The compatible-solute-binding protein OpuAC from *Bacillus subtilis*: ligand binding, site-directed mutagenesis, and crystallographic studies. *J. Bacteriol.* **190**, 5663–5671.
37. Horn, C., Sohn-Bosser, L., Breed, J., Welte, W., Schmitt, L. & Bremer, E. (2006). Molecular determinants for substrate specificity of the ligand-binding protein OpuAC from *Bacillus subtilis* for the compatible solutes glycine betaine and proline betaine. *J. Mol. Biol.* **357**, 592–606.
38. Schiefner, A., Holtmann, G., Diederichs, K., Welte, W. & Bremer, E. (2004). Structural basis for the binding of compatible solutes by ProX from the hyperthermophilic archaeon *Archaeoglobus fulgidus*. *J. Biol. Chem.* **279**, 48270–48281.
39. Kabsch, W. (1993). Automatic processing of rotation diffraction data from crystals of initially unknown symmetry and cell constants. *J. Appl. Crystallogr.* **26**, 795–800.
40. McCoy, A. J., Grosse-Kunstleve, R. W., Adams, P. D., Winn, M. D., Storoni, L. C. & Read, R. J. (2007). Phaser crystallographic software. *J. Appl. Crystallogr.* **40**, 658–674.
41. Laskowski, R. A., MacArthur, M. W., Moss, D. S. & Thornton, J. M. (1993). PROCHECK: a program to check the stereochemical quality of protein structures. *J. Appl. Crystallogr.* **26**, 283–291.
42. Panjikar, S., Parthasarathy, V., Lamzin, V. S., Weiss, M. S. & Tucker, P. A. (2005). Auto-Rickshaw: an automated crystal structure determination platform as an efficient tool for the validation of an X-ray diffraction experiment. *Acta Crystallogr. Sect. D*, **61**, 449–457.
43. Berntsson, R. P., Smits, S. H., Schmitt, L., Slotboom, D. J. & Poolman, B. (2010). A structural classification of substrate-binding proteins. *FEBS Lett.* **584**, 2606–2617.
44. Schiefner, A., Breed, J., Bösser, L., Kneip, S., Gade, J., Holtmann, G. *et al.* (2004). Cation–pi interactions as determinants for binding of the compatible solutes glycine betaine and proline betaine by the periplasmic ligand-binding protein ProX from *Escherichia coli*. *J. Biol. Chem.* **279**, 5588–5596.
45. Oswald, C., Smits, S. H., Höing, M., Sohn-Bösser, L., Dupont, L., Le Rudulier, D. *et al.* (2008). Crystal structures of the choline/acetylcholine substrate-binding protein ChoX from *Sinorhizobium meliloti* in the liganded and unliganded-closed states. *J. Biol. Chem.* **283**, 32848–33259.
46. Dougherty, D. A. (1996). Cation–pi interactions in chemistry and biology: a new view of benzene, Phe, Tyr, and Trp. *Science*, **271**, 163–168.
47. Tschapek, B., Pittelkow, M., Sohn-Bösser, L., Holtmann, G., Smits, S. H. J., Gohlke, H., Bremer, E. & Schmitt, L. (2011). Arg149 is involved in switching the low affinity, open state of the binding protein *Af*ProX into its high affinity, closed state. *J. Mol. Biol.* **411**, 36–52.
48. Quiocho, F. A. & Ledvina, P. S. (1996). Atomic structure and specificity of bacterial periplasmic receptors for active transport and chemotaxis: variation of common themes. *Mol. Microbiol.* **20**, 17–25.
49. Shilton, B. H. (2008). The dynamics of the MBP–MalFGK(2) interaction: a prototype for binding protein dependent ABC-transporter systems. *Biochim. Biophys. Acta*, **1778**, 1772–1780.
50. Cui, J., Qasim, S. & Davidson, A. L. (2010). Uncoupling substrate transport from ATP hydrolysis in the *Escherichia coli* maltose transporter. *J. Biol. Chem.* **285**, 39986–39993.
51. Kiran, M. D., Akiyoshi, D. E., Giacometti, A., Cirioni, O., Scalise, G. & Balaban, N. (2009). OpuC—an ABC transporter that is associated with *Staphylococcus aureus* pathogenesis. *Int. J. Artif. Organs*, **32**, 600–610.
52. Oswald, C., Smits, S. H., Höing, M., Bremer, E. & Schmitt, L. (2009). Structural analysis of the choline-binding protein ChoX in a semi-closed and ligand-free conformation. *Biol. Chem.* **390**, 1163–1170.
53. Dupont, L., Garcia, I., Poggi, M. C., Alloing, G., Mandon, K. & Le Rudulier, D. (2004). The *Sinorhizobium meliloti* ABC transporter Cho is highly specific for choline and expressed in bacteroids from *Medicago sativa* nodules. *J. Bacteriol.* **186**, 5988–5996.
54. Altschul, S. F., Madden, T. L., Schaffer, A. A., Zhang, J., Zhang, Z., Miller, W. & Lipman, D. J. (1997). Gapped BLAST and PSI-BLAST: a new generation of

protein database search programs. *Nucleic Acids Res.* **25**, 3389–3402.
55. Kokoeva, M. V., Storch, K. F., Klein, C. & Oesterhelt, D. (2002). A novel mode of sensory transduction in Archaea: binding protein-mediated chemotaxis towards osmoprotectants and amino acids. *EMBO J.* **21**, 2312–2322.
56. Thompson, J. D., Higgins, D. G. & Gibson, T. J. (1994). CLUSTAL W: improving the sensitivity of progressive multiple sequence alignment through sequence weighting, position-specific gap penalties and weight matrix choice. *Nucleic Acids Res.* **22**, 4673–4680.
57. Miller, J. H. (1992). *A Short Course in Bacterial Genetics. A Laboratory Manual and Handbook for Escherichia coli and Related Bacteria.* Cold Spring Harbor Laboratory, Cold Spring Harbor, NY.
58. Murshudov, G. N., Vagin, A. A. & Dodson, E. J. (1997). Refinement of macromolecular structures by the maximum-likelihood method. *Acta Crystallogr. Sect. D*, **53**, 240–255.